The Merging of a WDM Fiber-Radio Backbone with a 25 GHz WDM Ring Network

[1]Christina Lim, [1]Ampalavanapillai Nirmalathas, [1]Manik Attygalle, [2]Dalma Novak, and [2]Rod Waterhouse

[1]Australian Photonics Cooperative Research Centre, Photonics Research Laboratory,
Department of Electrical and Electronic Engineering,
The University of Melbourne, VIC 3010, Australia.
Tel: +61-3-8344-4486 Fax: +61-3-8344-6678 E-mail: c.lim@ee.mu.oz.au
[2]Corvis Subsea, Columbia MD 21046, USA.

Abstract — **We propose the merging of millimeter-wave broadband fiber-radio systems with WDM access networks at 25 GHz channel spacing. We investigate the performance characteristics of such fiber-radio systems experimentally and via simulation. The overall performance exhibits a penalty of < 2 dB.**

I. Introduction

Fixed wireless access technology operating at millimeter-wave (mm-wave) frequencies with optical fiber backhaul is an attractive solution for the future delivery of a variety of interactive broadband services [1]. It is therefore essential that mm-wave fiber-radio systems are able to merge or integrate with a WDM optical access network infrastructure. Fig. 1 shows such a merged access network incorporating a metropolitan area network (MAN) along with a number of mini switching centers servicing pico- or micro-cellular radio network architectures with a large number of base stations (BSs). Such fiber-radio networks need to be dimensioned so that a number of clusters of BSs are serviced by a switching node that assumes the role of a central office (CO) [2]. By doing so, WDM channels can be dropped or added into the optical WDM MAN network via the switching center in 25 GHz, 50 GHz, or 100 GHz blocks depending on the specifications of the WDM channel spacing.

In this paper, we present a new mm-wave fiber-radio system incorporating optical single sideband with carrier (OSSB+C) modulation [3] where an optical subcarrier multiplexed (SCM) scheme is used to feed a sectorized antenna interface. The proposed technique is capable of being integrated within existing WDM systems based on a 25 GHz channel spacing. The characteristics of the filter that drop and add a block of 25 GHz and the filter that extracts the optical local oscillator signal and the channel allocation for optimum system performance are investigated for the first time. The transmission performance of 8 WDM wavelengths with 32 SCM channels is also evaluated over 20 km of fiber in a ring architecture.

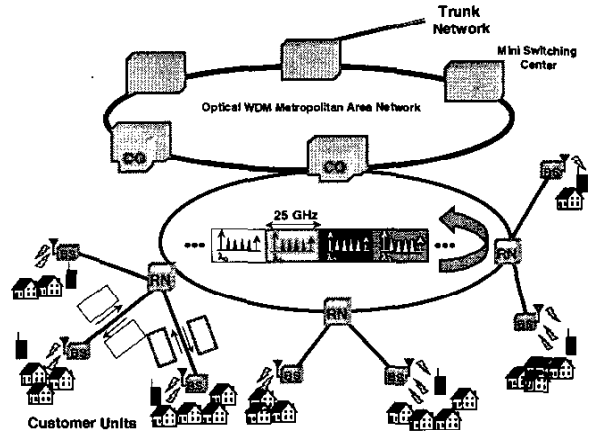

Fig. 1 Merging of optical WDM and broadband radio networks

II. Optimum Subcarrier Channel Allocation with Remote LO Delivery for a Four-Sector Antenna Interface

In Fig. 1, the MAN ring with a channel spacing of 25 GHz interconnects the mini switching center or CO to the remote nodes (RNs) where a number of BSs are connected in a star-tree configuration. Assuming each BS incorporates a four-sector antenna interface, each 25 GHz block comprises a single WDM channel with four SCM signals to drive four antenna sectors as well as a LO signal required for frequency translation at the BS [4]. Multiple blocks of 25 GHz containing the SCM channels are dropped from the MAN network via the CO and these blocks are distributed to the RNs. At the RN, a 25 GHz

0-7803-7695-1/03/$17.00 © 2003 IEEE

block will then be distributed to the designated BS to feed the sectorized antenna interface. Similarly in the upstream direction, signals from the different sectors can be arranged to fit within a 25 GHz bandwidth using either the same or different wavelength block and can be added back into the network before being routed to the trunk network. Such a proposed mm-wave fiber-radio system enables the use of standard WDM components within the CO, RNs and BSs, thus reducing the complexity and stringent requirements of the optical add-and-drop hardware.

In the proposed technique the subcarrier frequencies within a block are chosen to minimize intermodulation distortion (IMD) arising from the square-law process of the photodetector (assuming that any third-order nonlinearities resulting from the rf front-end have been eliminated). Fig. 1 shows the frequency allocation of the subcarriers within the 25 GHz block. The frequencies are chosen as: Channel 1 (Ch1) = 7 GHz, Channel 2 (Ch2) = 10 GHz, Channel 3 (Ch3) = 13 GHz and Channel 4 (Ch4) = 16 GHz while the LO signal is located at 23 GHz. This allocation ensures that the channels and the LO signal are fitted within a 25 GHz bandwidth and no IMD products fall within the channel bands after photodetection. A second stage upconversion is required at the base station with this arrangement to achieve the desired mm-wave frequency to drive each antenna sector.

III. Comparison of Theory and Experiment and Filter Characterization

Shown in Fig. 2 is the schematic for a single 25 GHz block and the SCM signal recovery at the RN and BS. At the RN, an optical bandpass filter (BPF) with a profile as shown in the inset A of Fig. 2, is required to drop the relevant 25 GHz block while an additional optical filter scheme with the profile as shown in inset B of Fig. 2 recovers the LO and information signals. The latter consists of two passbands of unequal amplitudes, where

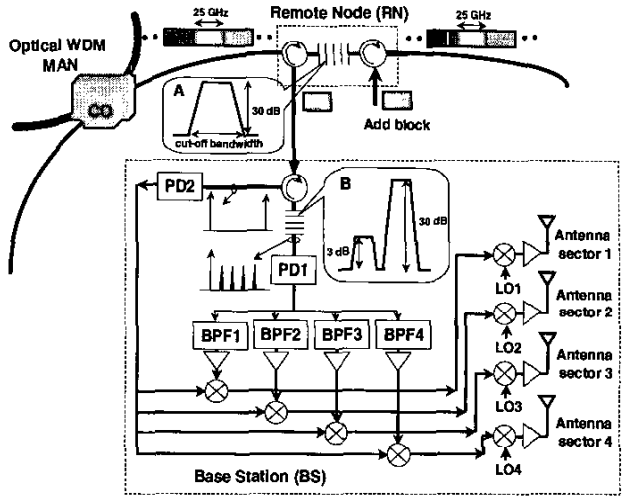

Fig. 2 Schematic for data recovery at BS for 25 GHz block

one passband recovers half of the optical carrier signal while the other recovers the LO signal entirely, as shown in inset B. The LO signal is recovered using photodetector 2 (PD2) and the radio channels are recovered using PD1. Individual data channels are isolated using an rf BPF and then upconverted using the recovered LO signal before undergoing a second stage upconversion (using lower microwave frequency LO signals of < 6 GHz) to the desired mm-wave frequency. The lower microwave frequency LO oscillators are labeled LO1, LO2, LO3 and LO4 in Fig. 2.

As a proof-of-concept experiment, three subcarrier channels at 7 GHz, 10 GHz and 13 GHz, with an LO signal at 23.1 GHz were transmitted over 10 km of single-mode fiber. Due to the limitations of the available rf bandpass filters, only 25 Mb/s of data was transmitted on each channel. The subcarrier signals and LO signal were received at the BS separately and the subcarriers were upconverted to 36 GHz, 37 GHz and 38 GHz,

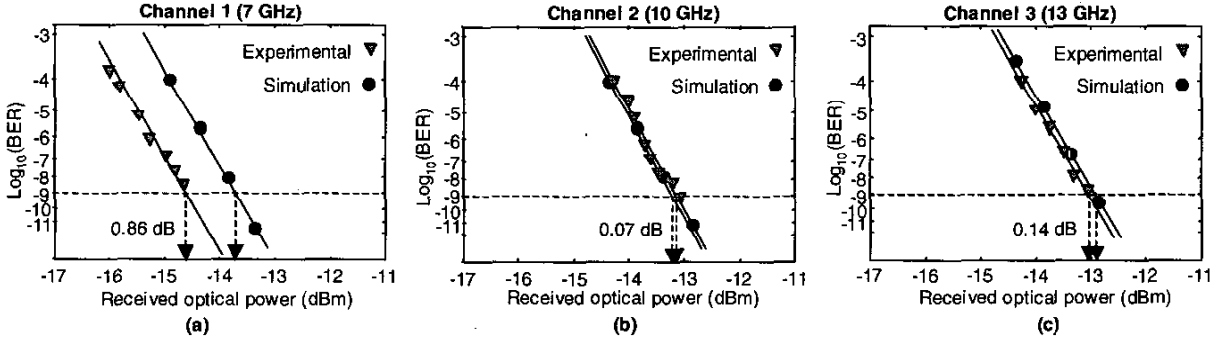

Fig. 3 Measured and simulated BER curves for 25 Mb/s recovered for (a) Ch1 (b) Ch2 and (c) Ch3

respectively. Figs. 3a-3c shows the measured bit-error-rate (BER) for each channel with the other channels transmitted simultaneously. Also shown are the predicted BER curves obtained using VPITransmissionMaker™ [5] with device parameters close to experimental values. The simulations show good agreement with experiment and the small discrepancy is attributed to experimental error.

It can be seen from Fig. 2 that the filter profile characteristics (25 GHz waveband add-drop filter and LO signal extraction filter) play an important role in the system performance. To characterize the 25 GHz filter, it is assumed that the filter has a trapezoidal profile with a fixed center frequency and 0 dB insertion loss bandwidth of 24 GHz. With reference to the inset A of Fig. 2, we define the cut-off bandwidth as the frequency where the signal magnitude is 30 dB down. Fig. 4a shows the predicted BER curves plotted as a function of 25 GHz filter cut-off bandwidth for all four channels. It can be seen that for all channels to be recovered error-free (BER $\leq 10^{-9}$), a cut-off bandwidth < 47.5 GHz is required. The BER of all channels increases steadily as the roll-off slope decreases which can be attributed to the imperfect filter response of the 25 GHz BPF not rejecting the carriers and LOs of the neighboring blocks. As described earlier, the second optical filter has 2 functions: to extract the LO; and to extract the rf sub-carrier signals. Thus, the filter arrangement allows half of the carrier and the entire LO signal to be reflected to PD2. The other half of the carrier is transmitted to PD1 with the signals containing the rf information. It is assumed there is a 30 dB rejection of the LO signal at PD1 and a similar rejection of the rf signals with information at PD2. It is also assumed that this filter has a trapezoidal profile with a 30 dB cut-off bandwidth 10 GHz greater than the 0 dB bandwidth for each sub-band (see Fig. 2 inset B). To investigate the LO filter characteristic, the 0 dB bandwidth of the filter is varied while maintaining the 25 GHz filter cut-off bandwidth fixed at 45 GHz. Fig. 4b shows the simulated BER curves for all the channels plotted as a function of the LO filter 0 dB bandwidth. The results show that all the channels are not affected by the filter bandwidth if the bandwidth is < 13 GHz. As the filter bandwidth increases beyond 13 GHz however, the Ch1 BER increases which is attributed to the first passband moving into the region of the Ch1 sideband and hence, reducing the optical power by 3 dB. In addition, the performance of Ch4 degrades dramatically as the bandwidth increases beyond 12.9 GHz, due to the second passband completely removing the Ch4 sideband.

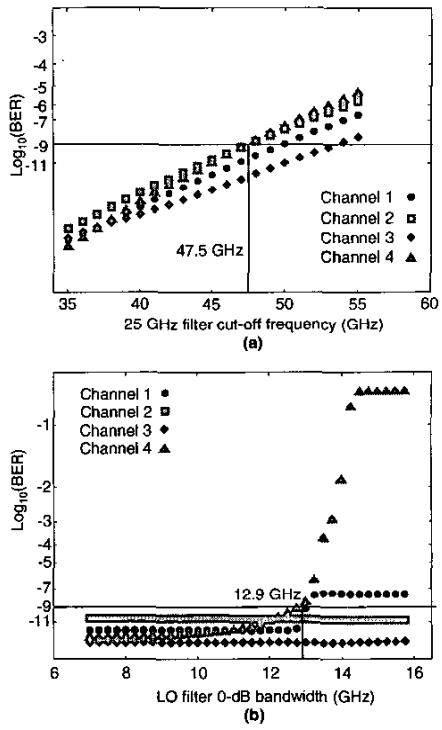

Fig. 4 BER curves for all channels as a function of (a) 25 GHz filter cut-off frequency (b) LO filter 0 dB bandwidth

IV. Simulation results for 8 WDM channel transmission for a four-sector antenna interface

To illustrate the proposed scheme, we simulated the transmission of 8 WDM channels each modulated with 4 SCM channels carrying 155 Mb/s binary-phased-shift-keyed (BPSK) data using the software package VPITransmissionMaker™. This simulates a WDM ring with a channel spacing of 25 GHz. The WDM channels were transmitted over 20 km of single-mode fiber before one of the middle blocks was dropped at the RN and subsequently distributed to the designated BS to feed a four-sector antenna interface. The cut-off frequency of the 25 GHz filter is set to 45 GHz while the 0 dB bandwidth of the LO signal filter is set to 12 GHz.

Figs. 5a-5d show the BERs for each received channel plotted as a function of average received optical power for a number of 25 GHz blocks, i.e. 1-8 blocks. The spread between the best and worst BER for the channels at a BER of 10^{-9} varies from 1.54 dB to 1.84 dB with Ch2 showing the greatest spread. The observed spread is mainly due to IMD introduced by the adjacent blocks when they are added into the system. However they remain unaffected when the number of adjacent blocks is greater than three,

which implies that the IMD contributions from adjacent blocks located on either side of the desired block are dominant with negligible contributions from other blocks.

V. Conclusions

We have proposed and investigated for the first time the distribution of radio signals in a mm-wave fiber-radio backbone with a sectorized antenna interface, when such a system is integrated in a standard WDM infrastructure with 25 GHz channel spacing. In addition, we characterized the optical filter for adding or dropping of the 25 GHz band and extracting the LO signal. It is shown that the filter requirements for such an application are not stringent and can be fabricated practically. Simulation investigations of multiple 25 GHz block transmissions in a ring network revealed that the proposed scheme has a penalty < 2 dB for all channels that can be attributed to IMD from adjacent blocks.

References

[1] R. Heidemann and G. Veith, "mm-wave photonic technologies for Gbit/s-wireless-local-loop", *Proc. OECC*, Chiba, Japan, pp. 310-311, Jun. 1998.

[2] A. Nirmalathas, C. Lim, D. Novak, R.B. Waterhouse, and D. Castleford, "The merging of photonic and radio technologies", *Proc. OECC*, Sydney, Australia, pp. 227-230, Jul. 2001.

[3] G.H. Smith, D. Novak, and Z. Ahmed, "Technique for optical SSB generation to overcome dispersion penalties in fibre-radio systems", *Electron. Lett.*, vol. 33, no. 1, pp. 74-75, 1997.

[4] C. Lim, A. Nirmalathas, D. Novak, R. Waterhouse, and G. Yoffe, "Millimeter-wave broadband fiber-wireless system incorporating baseband data transmission over fiber and remote LO delivery", *IEEE J. of Lightwave Technol.*, vol. 18, no. 10, pp. 1355-1363, Oct. 2000.

[5] VPIsystems™, http://www.VPIsystems.com.

Acknowledgement

The authors would like to thank Charlotte Marra for the fiber Bragg gratings used in the experiment.

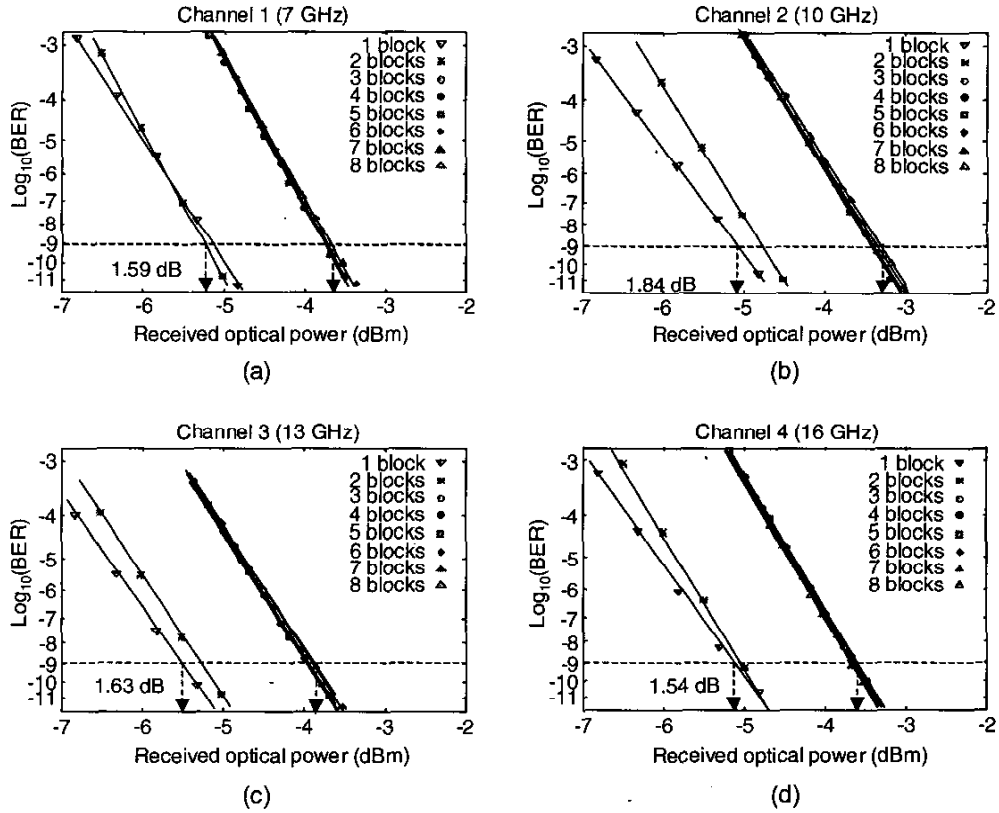

Fig. 5 BER curves for different number of transmission blocks for (a) Ch1 (b) Ch2 (c) Ch3 (d) Ch4